Inorg. Chem. **2008**, *47*, 9528−9536

Inorganic Chemistry
Article

Hydrothermal Synthesis, Structures, and Physical Properties of Four New Flexible Multicarboxylate Ligands-Based Compounds

Zhaorui Pan,[†] Hegen Zheng,*[,†,‡] Tianwei Wang,[†] You Song,[†] Yizhi Li,[†] Zijian Guo,[†] and Stuart R. Batten*[,§]

State Key Laboratory of Coordination Chemistry, School of Chemistry and Chemical Engineering, Nanjing National Laboratory of Microstructures, Nanjing University, Nanjing 210093, P.R. China, School of Chemistry, Monash University, Victoria, 3800, Australia, and State Key Laboratory of Structural Chemistry, Fujian Institute of Research on the Structure of Matter, Chinese Academy of Sciences, Fuzhou 350002, P.R. China

Received July 2, 2008

Four new compounds of partially or wholly deprotonated 5,5′-(1,4-phenylenebis(methylene))bis(oxy)diisophthalic acid (H_4L1) and 5,5′-(1,3-phenylenebis(methylene))bis(oxy)diisophthalic acid (H_4L2), namely $\{[Co(L1)_{0.5}]\cdot(H_2O)_2\}_n$ (**1**), $\{[Mn(L1)_{0.5}]\cdot(H_2O)_2\}_n$ (**2**), $\{[Cu(H_2L1)](\mu_2\text{-bipy})\}_n$ (bipy = 4, 4′-bipyridyl) (**3**), and $\{[Zn_2(L2)].H_2O\}_n$ (**4**) were synthesized in the presence or absence of auxiliary bipy ligand. Their structures have been determined by single-crystal X-ray diffraction analysis and further characterized by elemental analysis, IR spectra, and thermogravimetric analysis. Compounds **1** and **2** are isostructural and possess three-dimensional (3D) networks. In compound **3**, multicarboxylate ligands and bipy ligands link Cu centers to generate a two-dimensional (2D) sheet structure which is further connected by intermolecular hydrogen bonds to form a 3D supramolecular structure. In compound **4**, the Zn centers are connected by $L2^{4-}$ anions to generate a 3D framework. Magnetic susceptibility measurements indicate that compounds **1** and **2** exhibit antiferromagnetic coupling between adjacent Co(II) ions and Mn(II) ions. The photoluminescent properties of the free H_4L1 and H_4L2 ligands and compound **4** have been studied in the solid state at room temperature. Both ligands and compound **4** exhibit strong violet emissions. Compared with the fluorescent emission of the ligand, the emission of **4** is red-shifted and enhanced.

Introduction

The rational design and synthesis of functional coordination architectures have recently been extensively explored not only because of their intriguing variety of architectures[1−4] but also because of their potential functional properties such as magnetism,[5,6] photoluminescence,[7,8] hydrogen storage,[9−11] and catalysis.[12,13] An effective and facile method for the design of two-dimensional (2D) and three-dimensional (3D) metallosupramolecular species is still the appropriate

* To whom correspondence should be addressed. E-mail: zhenghg@nju.edu.cn (H.Z.), stuart.batten@sci.monash.edu.au (S.R.B.). Fax: 86-25-83314502.

† Nanjing University.

‡ Fujian Institute of Research on the Structure of Matter, Chinese Academy of Sciences.

§ Monash University.

(1) (a) Yaghi, O. M.; Li, H. L.; Davis, C.; Richardson, D.; Groy, T. L. *Acc. Chem. Res.* **1998**, *31*, 474–484. (b) Li, H.; Eddaoudi, M.; O'Keeffe, M.; Yaghi, O. M. *Nature.* **1999**, *402*, 276–279. (c) Chen, B. L.; Eddaoudi, M.; Reineke, T. M.; Kampf, J. W.; O'Keeffe, M.; Yaghi, O. M. *J. Am. Chem. Soc.* **2000**, *122*, 11559–11561. (d) Eddaoudi, M.; Li, H. L.; Yaghi, O. M. *J. Am. Chem. Soc.* **2000**, *122*, 1391–1397. (e) Eddaoudi, M.; Moler, D. B.; Li, H.; Chen, B. L.; Reineke, T. M.; O'Keeffe, M.; Yaghi, O. M. *Acc. Chem. Res.* **2001**, *34*, 319–330. (f) Ockwig, N. W.; Delgado-Friedrichs, O.; O'Keeffe, M.; Yaghi, O. M. *Acc. Chem. Res.* **2005**, *38*, 176–182.

(2) (a) Kondo, M.; Yoshitomi, T.; Seki, K.; Matsuzaka, H.; Kitagawa, S. *Angew. Chem., Int. Ed. Engl.* **1997**, *36*, 1725–1727. (b) Noro, S. I.; Kitagawa, S.; Kondo, M.; Seki, K. *Angew. Chem., Int. Ed.* **2000**, *39*, 2081–2084.

(3) (a) Walton, K. S.; Snurr, R. Q. *J. Am. Chem. Soc.* **2007**, *129*, 8552–8556. (b) Wang, G. M.; Li, J. H.; Huang, H. L.; Li, H.; Zhang, J. *Inorg. Chem.* **2008**, *47*, 5039–5041. (c) Li, M. X.; Miao, Z. X.; Shao, M.; Liang, S. W.; Zhu, S. R. *Inorg. Chem.* **2008**, *47*, 4481–4489.

(4) Seo, J. S.; Whang, D.; Lee, H.; Jun, S. I.; Oh, J.; Jeon, Y. J.; Kim, K. *Nature* **2000**, *404*, 982–986.

(5) (a) Kahn, O. *Molecular Magnetism*; VCH: Weinheim, Germany, 1993. (b) Turnbull, M. M.; Sugimoto, T.; Thompson, L. K. *Molecule-Based Magnetic Materials*; American Chemical Society: Washington, DC, 1996. (c) Mathoniere, C.; Sutter, J. P.; Yakhmi, J. V. In *Magnetism: Molecules to Materials II*; Miller, J. S., Drillon, M., Eds.; Wiley-VCH: Weinheim, Germany, 2003; pp 1−44.

(6) (a) Karmakar, T. K.; Ghosh, B. K.; Usman, A.; Fun, H. K.; Rivière, E.; Mallah, T.; Aromì, G.; Chandra, S. K. *Inorg. Chem.* **2005**, *44*, 2391–2399. (b) Du, M.; Bu, X. H.; Guo, Y. M.; Ribas, J. *Chem.—Eur. J.* **2004**, *10*, 1345–1354.

10.1021/ic801221r CCC: $40.75
Published on Web 09/24/2008

choice of well-designed organic ligands as bridges or terminal groups (building blocks) with metal ions or metal clusters as nodes.[14] Among various organic ligands, multicarboxylate ligands are often selected as multifunctional organic linkers because of their abundant coordination modes to metal ions, resulting from completely or partially deprotonated sites, allowing for various structural topologies,[15] and also because of their ability to act as H-bond acceptors and donors to assemble supramolecular structures.[16] For example, aromatic multicarboxylates (benzene dicarboxylate, benzene tricarboxylate, 4,4′-oxybis(benzoate), and ethylenedi(4-oxybenzoate)) have been investigated widely for the design and synthesis of open framework complexes. However, the flexible ligand 5,5′-(1,4-phenylenebis(methylene))bis(oxy)diisophthalic acid (H_4L1) has not been explored up to now, and only one compound $[Cu_{24}(L_2)_{12}(H_2O)_{16}(DMSO)_8]n$ constructed from 5,5′-(1,3-phenylenebis(methylene))bis(oxy)diisophthalic acid (H_4L2) was synthesized recently.[17]

Many topologies can be obtained by incorporating flexible linker units into our bridging ligands to access diverse architectures. Such linkers can be single-atom spacers, such as methylene groups or ether oxygen atoms, or longer spacers, such as three-atom propylene groups.[18,19] In this paper, we designed and synthesized two flexible and multidentate ligands H_4L1 and H_4L2, which have two benzene dicarboxylate substituents attached to a central benzene ring through two-atom flexible spacer groups. These two ligands have four obvious characteristics: (1) Both ligands can completely or partially deprotonated and adopt various coordination modes when they coordinate to metals and thus may produce various structural topologies, owing to their tetradentate carboxylate arms and their flexible structures; (2) They can act not only as a hydrogen bond acceptors but also as a hydrogen bond donors, depending on the degree of deprotonation; (3) The carboxylic groups can propagate magnetic superexchange between metal centers; (4) They have a large conjugated π-systems and therefore can combine with d^{10} metals to construct useful photoluminescence materials. With the aim of understanding the coordination chemistry of these two versatile ligands and preparing new porous materials with interesting structural topologies and physical properties, we chose H_4L1 and H_4L2 as bridging ligands to react with the d-block metal ions Co(II), Mn(II), and Zn(II), and successfully synthesized compounds **1**, **2**, and **4**. In the presence of the auxiliary bipy ligand, H_4L1 reacted with Cu(II) to give compound **3**. The details of their syntheses, structures, and physical properties are reported below.

Experimental Section

Materials and Methods. H_4L1 and H_4L2 ligands were prepared according to the literature.[20] All other chemicals were of reagent grade quality from commercial sources and were used without further purification. The IR absorption spectra of the compounds were recorded in the range of 400−4000 cm^{-1} by means of a Nicolet (Impact 410) spectrometer with KBr pellets (5 mg of sample in 500 mg of KBr). C, H, and N analyses were carried out with a Perkin-Elmer 240C elemental analyzer. Luminescent spectra were recorded with a SHIMAZU VF-320 X-ray fluorescence spectrophotometer at room temperature (25 °C). X-ray diffraction (XRD) measurements were performed on a Philips X′pert MPD Pro X-ray diffractometer using Cu Kα radiation (0.15418 nm), in which the X-ray tube was operated at 40 kV and 40 mA. The as-synthesized samples were characterized by thermogravimetric analysis (TGA) on a Perkin-Elmer thermogravimetric analyzer Pyris 1 TGA up to

(7) (a) Li, M.; Xiang, J. F.; Yuan, L. J.; Wu, S. M.; Chen, S. P.; Sun, J. T. *Cryst. Growth Des.* **2006**, *6*, 2036–2040. (b) Pang, J.; Marcotte, E. J. P.; Seward, C.; Brown, R. S.; Wang, S. *Angew. Chem., Int. Ed.* **2001**, *40*, 4042–4045. (c) Zheng, S. L.; Yang, J. H.; Yu, X. L.; Chen, X. M.; Wong, W. T. *Inorg. Chem.* **2004**, *43*, 830–838. (d) He, J. H.; Yu, J. H.; Zhang, Y. T.; Pan, Q. H.; Xu, R. R. *Inorg. Chem.* **2005**, *44*, 9279–9282. (e) Zhang, X. M.; Tong, M. L.; Gong, M. L.; Chen, X. M. *Eur. J. Inorg. Chem.* **2003**, 138–142.

(8) (a) Bauer, C. A.; Timofeeva, T. V.; Settersten, T. B.; Patterson, B. D.; Liu, V. H.; Simmons, B. A.; Allendorf, M. D. *J. Am. Chem. Soc.* **2007**, *129*, 7136–7144. (b) Fang, Q. R.; Zhu, G. S.; Jin, Z.; Ji, Y. Y.; Ye, J. W.; Xue, M.; Yang, H.; Wang, Y.; Qiu, S. L. *Angew. Chem., Int. Ed.* **2007**, *46*, 6638–6642.

(9) (a) Kondo, M.; Okubo, T.; Asami, A.; Noro, S. I.; Yoshitomi, T.; Kitagawa, S.; Ishii, T.; Matsuzaka, H. *Agnew. Chem., Int. Ed.* **1999**, *38*, 140–143. (b) Kitagawa, S.; Kitaura, R.; Noro, S. I. *Angew. Chem., Int. Ed.* **2004**, *43*, 2334–2375. (c) Matsuda, R.; Kitaura, R.; Kitagawa, S.; Kubota, Y.; Belosludov, R. U.; Kobayashi, T. C.; Sakamoto, H.; Chiba, T.; Takata, M.; Kawazoe, Y.; Mita, Y. *Nature* **2005**, *436*, 238–241.

(10) (a) Rosi, N. L.; Eckert, J.; Eddaoudi, M.; Vodak, D. J.; Kim, J.; O'Keeffe, M.; Yaghi, O. M. *Science* **2003**, *300*, 1127–1129. (b) Li, H.; Eddaoudi, M.; O'Keeffe, M.; Yaghi, O. M. *Nature* **2005**, *402*, 276–279. (c) Roswell, J. L. C.; Yaghi, O. M. *Agnew. Chem., Int. Ed.* **2005**, *44*, 4670–4679. (d) Sudik, A. C.; Millward, A. R.; Ockwig, N. W.; Cote, A. P.; Kim, J.; Yaghi, O. M. *J. Am. Chem. Soc.* **2005**, *127*, 7110–7118.

(11) (a) Ferey, G.; Latroche, M.; Serre, C.; Millange, F.; Loiseau, T.; Percheron-Guegan, A. *Chem. Commun.* **2003**, 2976–2977. (b) Zhao, X.; Xiao, B.; Fletcher, A. J.; Thomas, K. M.; Bradshaw, D.; Rosseinsky, M. J. *Science* **2004**, *306*, 1012–1015. (c) Pan, L.; Holson, D.; Ciemnolonski, L. R.; Heddy, R.; Li, J. *Angew. Chem., Int. Ed.* **2006**, *46*, 616–619. (d) Dinca, M.; Yu, A. F.; Long, J. R. *J. Am. Chem. Soc.* **2006**, *128*, 8904–8913.

(12) Adams, R. D.; Cotton, F. A. *Catalysis by Di- and Polynuclear Metal Cluster Complexes*; Wiley-VCH: New York, 1998.

(13) (a) Fujita, M.; Kwon, Y. J.; Washizu, S.; Ogura, K. *J. Am. Chem. Soc.* **1994**, *116*, 1151–1152. (b) Kesanli, B.; Lin, W. B. *Coord. Chem. Rev.* **2003**, *246*, 305–326. (c) Rowsell, J. L. C.; Yaghi, O. M. *Angew. Chem., Int. Ed.* **2005**, *44*, 4670–4679. (d) Wong-Foy, A. G.; Matzger, A. J.; Yaghi, O. M. *J. Am. Chem. Soc.* **2006**, *128*, 3494–3495. (e) Pan, L.; Sander, M. B.; Huang, X. Y.; Li, J.; Smith, M.; Bittner, E.; Bockrath, B.; Johnson, J. K. *J. Am. Chem. Soc.* **2004**, *126*, 1308–1309.

(14) (a) Hoskins, B. F.; Robson, R. *J. Am. Chem. Soc.* **1990**, *112*, 1546–1554. (b) Robson, R. *J. Chem. Soc., Dalton Trans.* **2000**, 3735–3744.

(15) (a) Janiak, C. *Dalton Trans.* **2003**, *3*, 2781–2804. (b) Evans, O. R.; Lin, W. *Acc. Chem. Res.* **2002**, *35*, 511–522. (c) Ockwig, N. W.; Delgado-Friedrichs, O.; O'Keeffe, M.; Yaghi, O. M. *Acc. Chem. Res.* **2005**, *38*, 176–182. (d) Batten, S. R.; Robson, R. *Angew. Chem., Int. Ed.* **1998**, *37*, 1460–1494. (e) Rao, C. N. R.; Natarajan, S.; Vaidhyanathan, R. *Angew. Chem., Int. Ed.* **2004**, *43*, 1466–1496. (f) Kitagawa, S.; Kitaura, R.; Noro, S. I. *Angew. Chem., Int. Ed.* **2004**, *43*, 2334–2375. (g) Blatov, V. A.; Carlucci, L.; Ciani, G.; Proserpio, D. M. *CrystEngComm* **2004**, *6*, 378–395.

(16) (a) Moulton, B.; Zaworotko, M. *Chem. Rev.* **2001**, *101*, 1629–1658. (b) Du, M.; Jiang, X. J.; Zhao, X. J. *Inorg. Chem.* **2006**, *45*, 3998–4006. (c) Paz, F. A. A.; Klinowski, J. *Inorg. Chem.* **2004**, *43*, 3882–3893. (d) Abourahma, H.; Moulton, B.; Kravtsov, V.; Zaworotko, M. J. *J. Am. Chem. Soc.* **2002**, *124*, 9990–9991. (e) Wang, R.; Hong, M.; Luo, J.; Cao, R.; Shi, Q.; Weng, J. *Eur. J. Inorg. Chem.* **2002**, 2904–2912. (f) Biradha, K. *CrystEngComm* **2003**, *5*, 374–384. (g) Varughese, S.; Pedireddi, V. R. *Chem.—Eur. J.* **2006**, *12*, 1597–1609. (h) Wang, J.; Lin, Z. J.; Ou, Y. C.; Yang, N. L.; Zhang, Y. H.; Tong, M. L. *Inorg. Chem.* **2008**, *47*, 190–199.

(17) Perry, J. J., IV.; Kravtsov, V. C.; McManus, G. J.; Zaworotko, M. J. *J. Am. Chem. Soc.* **2007**, *129*, 10076–10077.

(18) Steel, P. J. *Acc. Chem. Res.* **2005**, *38*, 243–250.

(19) McMorran, D. A.; Pfadenhauer, S.; Steel, P. J. *Aust. J. Chem.* **2002**, *55*, 519–522.

(20) Pan, Y. J.; Ford, W. T. *J. Org. Chem.* **1999**, *64*, 8588–8593.

Table 1. Crystallographic Data and Structure Refinement Details for Compounds **1**−**4**

compound	**1**	**2**	**3**	**4**
formula	$C_{12}H_{11}CoO_7$	$C_{12}H_{11}MnO_7$	$C_{34}H_{24}CuN_2O_{10}$	$C_{24}H_{16}Zn_2O_{11}$
formula weight	326.14	322.15	684.09	611.11
crystal system	monoclinic	monoclinic	monoclinic	monoclinic
space group	*C*2/*c*	*C*2/*c*	*C*2/*c*	*C*2/*c*
a (Å)	20.282(4)	20.607(4)	12.872(3)	18.392(4)
b (Å)	15.220(3)	15.384(3)	11.015(2)	16.462(4)
c (Å)	7.9736(17)	8.1417(17)	20.869(4)	7.6238(17)
β (deg)	106.461(3)	107.167(3)	102.120(4)	90.345(3)
V (Å^3)	2360.4(9)	2466.0(9)	2892.9(10)	2297.3(9)
Z	8	8	4	4
D_c (g cm^{-3})	1.836	1.735	1.571	1.767
μ(Mo Ka)(mm^{-1})	1.485	1.101	0.823	2.153
F(000)	1328	1312	1404	1232
temperature(K)	293	293	291	291
theta min-max (deg)	2.09, 25.00	2.07, 25.00	2.00, 25.99	1.66, 25.99
tot., uniq. data	5728, 2065	6002, 2175	7617, 2845	6125, 2255,
R(int)	0.0537	0.0511	0.0294	0.0320
observed data [$I > 2\sigma(I)$]	1868	1784	2484	1805
Nref, Npar	2065, 181	2175, 181	2845, 218	2255, 178
R1, wR2 (all data)	0.0356, 0.1004	0.0500, 0.1074	0.0476, 0.1097	0.0694, 0.1081
S	1.007	1.003	1.086	1.057
min. and max resd dens (e·Å^{-3})	−0.406, 0.068	−0.547, 0.065	−0.240, 0.207	−0.531, 0.075

1023 K using a heating rate of 20 K min^{-1} under a N_2 atmosphere. Temperature dependent magnetic susceptibility data for polycrystalline compounds **1** and **2** were obtained on a SQUID magnetometer under an applied field of 2000 Oe over the temperature range of 2−300 K. Diamagnetic correction is considered as part of the data analysis by the generalized molar susceptibility expression

$$\chi_m = \chi_{Co} + \chi_{dia} \quad (1)$$

where χ_m is the observed molar susceptibility of compound **1**, χ_{Co} is the temperature-dependent paramagnetic susceptibility of the Co(II) ion, and χ_{dia} is the diamagnetic correction according to the data that have been tabulated[21] as Pascal's constants and constituent corrections. Brunauer−Emmett−Teller (BET) surface areas and pore-size distributions were measured using a Micromeritics ASAP2000 adsorption analyzer.

Synthesis. Synthesis of {[Co(L1)$_{0.5}$]·(H$_2$O)$_2$]}$_n$ (1). A mixture of H_4L1 (12 mg, 0.025 mmol), KOH (3 mg, 0.05 mmol), $CoCl_2 \cdot 6H_2O$ (12 mg, 0.05 mmol), and H_2O (7 mL) was sealed in a 15-mL PTFE-lined stainless-steel acid digestion bomb and heated at 160 °C for 5 days and then was cooled to give violet crystals of compound **1** together with some unrecognized pink polycrystalline material, which were isolated by filtration, and washed with water. The sample was allowed to air-dry. Yield: 12.39 mg (76%) yield based on metal. Anal. Calcd for $C_{12}H_{11}CoO_7$: C, 44.19%; H, 3.40%. Found: C, 44.30%; H, 3.28%. IR (KBr, cm^{-1}): 3422(w), 3084(w), 1624(m), 1542(s), 1458(S), 1382(vs), 1324(m), 1264(m), 1244(m), 1132(w), 1040(m), 1024(w), 823(m), 779(m), 724(m), 466(w).

Synthesis of {[Mn(L1)$_{0.5}$]·(H$_2$O)$_2$]}$_n$ (2). Similar to the preparation of **1**, a hydrothermal reaction of H_4L1 (12 mg, 0.025 mmol), KOH (3 mg, 0.05 mmol), $Mn(OAc)_2 \cdot 4H_2O$ (12 mg, 0.05mmol), and H_2O (7 mL) was sealed in a 15-mL PTFE-lined stainless-steel acid digestion bomb and heated at 160 °C for 5 days. The final product contained large quantities of yellow crystals of **2**, which were filtered off, washed with copious quantities of distilled water, and dried under ambient conditions. Yield: 11.60 mg (72%) yield based on metal. Anal. Calcd for $C_{12}H_{11}MnO_7$: C, 44.74%; H, 3.44%. Found: C, 44.68%; H, 3.51%. IR (KBr, cm^{-1}): 3449(s), 2975(W), 2363(W), 1627(s), 1542(s), 1458(S), 1382(s), 1322(m), 1262(m), 1242(m), 1131(w), 1039(m), 885(w), 821(m), 779(m), 722(m), 466(w).

Synthesis of {[Cu(H$_2$L1)](μ_2-bipy)}$_n$ (3). A mixture of H_4L1 (12 mg, 0.025 mmol), bipy (4 mg, 0.025 mmol), $Cu(OAc)_2 \cdot 4H_2O$ (12 mg, 0.05 mmol), and H_2O (7 mL) was sealed in a 15-mL PTFE-lined stainless-steel acid digestion bomb and heated at 160 °C for 5 days and then was cooled to give little red block crystals of **3** and large quantities of gray powder. **3** was isolated by filtration, washed with copious quantities of distilled water, and dried under ambient conditions. Anal. Calcd for $C_{34}H_{24}CuN_2O_{10}$: C, 59.69%; H, 3.54%; N, 4.09%. Found: C, 59.80%; H, 3.59%; N, 4.02%. IR(KBr, cm^{-1}): 3445(s), 1708(s), 1610(s), 1437(m), 1422(m), 1385(s), 1370(s), 1332(m), 1262(m), 1118(m), 1104(m), 1058(s), 824(m), 678(m), 498(w).

Synthesis of {[Zn$_2$(L2)].H$_2$O}$_n$ (4). A mixture of H_4L2 (12 mg, 0.025 mmol), KOH (5 mg, 0.1 mmol), $Zn(NO_3)2 \cdot 6H_2O$ (12 mg, 0.05mmol), and H_2O (7 mL) was sealed in a 15-mL PTFE-lined stainless-steel acid digestion bomb and heated at 160 °C for 6 days and then was cooled to give large quantities of white crystals of **4**, which were obtained by filtration and washed with water. The sample was allowed to air-dry. Yield: 12.22 mg (80%) yield based on metal. Anal. Calcd for $C_{24}H_{16}O_{11}Zn_2$: C, 47.17%; H, 2.64%. Found: C, 47.26%; H, 2.72%. IR(KBr, cm^{-1}): 3429(vs), 1628(m), 1555(s), 1525(s), 1458(s), 1385(vs), 1327(m), 1273(s), 1157(ws), 1135(m), 1070(m), 782(m),716(m), 578(ws).

X-ray Crystallography. Single crystals of **1**−**4** were prepared by the methods described in the synthetic procedure. X-ray crystallographic data of **1**−**4** were collected at room temperature using epoxy-coated crystals mounted on glass fiber. All measurements were made on a Bruker Apex Smart CCD diffractometer with graphite-monochromated Mo Kα radiation (λ = 0.71073 Å). The structures of compounds **1**, **2**, and **4** were solved by direct methods, while compound **3** was solved by the heavy atom method, and the non-hydrogen atoms were located from the trial structure and then refined anisotropically with SHELXTL using a full-matrix least-squares procedures based on F^2 values.[22] The hydrogen atom positions were fixed geometrically at calculated distances and allowed to ride on the parent atoms. The relevant crystallographic data are presented in Table 1, while the selected bond lengths and angles are given in Supporting Information, Table S1.

(21) Boudrcaux, E. A.; Mulay, L. N. *Theory and Applications of Molecular Paramagnetism*; Wiley-Interscience: New York, 1976; p 477 ff.
(22) *Bruker 2000, SMART (Version 5.0), SAINT-plus (Version 6), SHELXTL (Version 6.1), and SADABS (Version 2.03)*; Bruker AXS Inc.: Madison, WI.

Results and Discussion

Synthesis and IR Spectrum. Hydrothermal synthesis under pressure and at low temperatures (100−200 °C) is a straightforward and effective method for the preparation of metal-organic coordination polymers.[23] The hydrothermal reaction of H_4L1 with $CoCl_2 \cdot 6H_2O$ gave violet crystals of compound **1** together with some unrecognized pink polycrystalline material. In the case of Mn^{2+}, compound **2** appears as a pure phase in 72% yield. Compound **3** appears as a minor phase. Compound **4** appears as a pure phase in 80% yield. It should also be pointed out that compounds **1**, **2**, and **4** were highly reproducible for repeated synthesis under the reaction conditions employed in this work. However, compound **3** was difficult to reproduce and only characterized by single X-ray crystallography, IR spectra, and elemental analysis. The IR spectra of these compounds show the characteristic bands of the $L1^{4-}$, $[H_2L1]^{2-}$, or $L2^{4-}$ at 1630−1555 cm^{-1} for the asymmetric vibration and at 1454−1348 cm^{-1} for the symmetric vibration. The broad bands at 3530−3400 cm^{-1} are assigned to the stretching vibrations of COOH groups and H_2O molecules. The absence of absorption bands at 1720−1690 cm^{-1} in **1**, **2**, and **4** indicates the H_4L1 or H_4L2 ligand adopts the completely deprotonated $L1^{4-}$ or $L2^{4-}$ form, whereas the presence of strong peaks at 1708 cm^{-1} for **3** suggests the H_4L1 ligand adopts the partly deprotonated $[H_2L1]^{2-}$ form, which is consistent with the X-ray structural analysis. The Supporting Information, Figure S1 shows the three coordination modes of $L1^{4-}$, $L2^{4-}$ and H_2L1^{2-} observed in this work.

Crystal Structures. Crystal Structures of 1 and 2. Single-crystal X-ray diffraction analyses reveal that **1** and **2** are isostructural and crystallize in the monoclinic *C*2/*c* space group, and thus only structure **1** will be discussed here. As shown in Figure 1a, compound **1** consists of one kind of Co(II) cation, which adopts a slightly distorted octahedral geometry, coordinated by four carboxylate oxygen atoms (O1#2, O2#2, O5, O7#3) from three different $L1^{4-}$ anions [Co−O:2.0200(18)−2.2643(17)Å;O−Co−O,60.11(6)−161.13(6)°], and two water molecules (O3, O4) [Co1−O3: 2.1418(18) Å; Co1−O4: 2.0740(17) Å; O4−Co1−O3: 87.52(7)°]. The aryloxy groups along each arm of the H_4L1 ligands are indeed twisted at an angle of 50.21(2)° away from the plane of the central benzene ring in compound **1**. H_4L1 ligand adopts the completely deprotonated $L1^{4-}$ form and acts as an octadentate-chelating ligand. Four deprotonated carboxylate groups of the $L1^{4-}$ anion adopt two kinds of coordination modes (Supporting Information, Figure S1a). Two carboxylate groups of opposite sides of the aryloxy group adopt bis-monodentate coordination modes to bridge two Co centers with the Co···Co distance of 4.7849(9) Å, whereas another two carboxylate groups coordinate to the same Co centers by adopting chelating coordination modes.

Each $L1^{4-}$ ligand coordinates to six Co(II) cations (Supporting Information, Figure S1a) and each Co(II) cation connects with three $L1^{4-}$ anions to form a 3D network. The distortion of the aryloxy groups along each arm of the H_4L1 ligand from the plane of the central benzene ring results in a 3D channelled structure with three parallel tunnels along the *c* axis: A, B, and C (Figure 1b). All the channels are empty. In addition, the 3D structure is further stabilized by hydrogen bonds between coordinated water molecules and carboxylate O atoms (Supporting Information, Table S2).

A better insight into the nature of this intricate framework can be achieved by the application of a topological approach, reducing multidimensional structures to simple node and connection nets. The Co(II) centers can be regarded as 3-connected nodes and all crystallographical independent $L1^{4-}$ ligands act as 6-connected nodes. Therefore, the whole structure can thus be represented as a $(4^2.8)_2(4^4.6^2.8^8.10)$ net, as displayed in Figure 1c.

Crystal Structure of $\{[Cu(H_2L1)](\mu_2\text{-bipy})\}_n$ (3). The asymmetric unit of **3** contains one Cu^{2+} cation, one bipy ligand, and one H_2L1^{2-} anion. As shown in Figure 2a, all Cu atoms are six-coordinated by two nitrogen atoms from two bipy ligands and four oxygen atoms from two $H_2L_1^{2-}$ anions, forming a slightly distorted octahedral geometry. The distances of Cu1−O1, Cu1−O2, Cu1−N1, and Cu1−N2#2 are 1.9552(19) Å, 2.5606(20) Å, 1.991(3) Å, and 1.973(3) Å, respectively. The angle of N2#2−Cu1−N1 is 180.0(1)°. In compound **3**, the H_4L1 ligands only partially deprotonate. Each deprotonated carboxylate group of H_2L1^{2-} acts as a bis-monodentate ligand (Supporting Information, Figure S1b) to bridge two Cu(II) ions affording a uniform chain. These chains are further cross-linked by bridging bipy ligands along the *c* axis to generate a 2D rectangular grid layer with a 20.54 Å × 11.02 Å window (Figure 2b). The two protonated carboxylate groups of the H_2L1^{2-} motif contribute to the stabilization of the structure through extensive hydrogen bonds with the coordinated carboxylate oxygen atoms. The adjacent layers are thus cross-linked into a 3D network (Figure 2c, Supporting Information, Table S2).

Crystal Structure of $\{[Zn_2(L2)].H_2O\}_n$ (4). The Zn(II) atom is coordinated by four oxygen atoms from four $L2^{4-}$ anions in a distorted tetrahedral arrangement, with the Zn−O distance ranging from 1.929(3) Å to 1.960(3) Å. The aryloxy groups along each arm of the H_4L2 ligands are only slightly twisted at an angle of 6.199(1)° away from the plane of the central benzene ring in compound **4**. The ligand, with a syn conformation, adopts a completely deprotonated $L2^{4-}$ form and acts as an octadentate ligand. The deprotonated carboxylate groups of the $L2^{4-}$ anion all adopt bis-monodentate coordination modes to bridge two Zn centers. Each $L2^{4-}$ group thus coordinates to eight Zn(II) cations (Supporting Information, Figure S1c) and each Zn(II) cation connects with three $L2^{4-}$ anions giving rise to a 3D structure containing three parallel channels along the *c* axis: square-shaped A, B, and nanoscaled channel C with dimensions of 10.24 Å × 14.75 Å (Figure 3b,c). Channels A and B are empty, whereas channel C is occupied by guest water molecules. In addition, the 3D structure is further stabilized by hydrogen bonds between water molecules and carboxylate

(23) (a) Lu, J. Y.; Runnels, K. R. *Inorg. Chem. Commun.* **2001**, *4*, 678–681. (b) Lu, J. Y.; Schauss, V. *Eur. J. Inorg. Chem.* **2002**, 1945–1947. (c) Lu, J. Y.; Babb, A. M. *Inorg. Chem.* **2002**, *41*, 1339–1341.

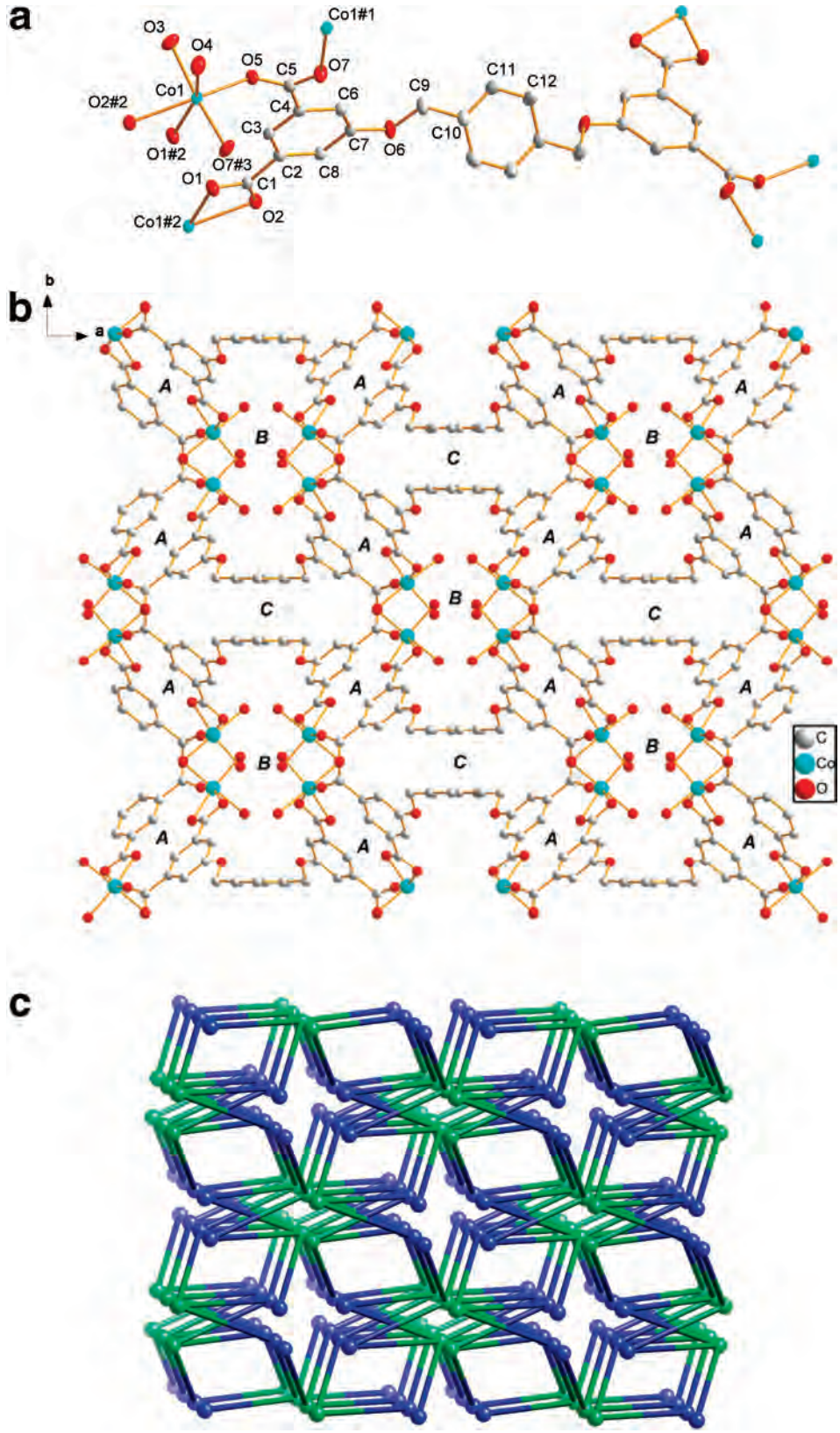

Figure 1. (a) Thermal Ellipsoid Plot (ORTEP) drawing of **1** showing 30% ellipsoid probability (hydrogen atoms are omitted for clarity). Symmetry codes: #1 = x, $-y$, 0.5 + z; #2 = 0.5 − x, 0.5 − y, − z; #3 = x, $-y$, −0.5 + z. (b) A view of three kinds of channels of compound **1** along the c axis (hydrogen atoms are omitted for clarity). (c) Schematic representation of the topology of compound **1**. Blue nodes represent Co atoms and green nodes represent $L1^{4-}$ ligands.

O atoms (Supporting Information, Table S2). From a topological viewpoint, the Zn(II) centers can be viewed as 4-connecting nodes, and all crystallographically independent $L2^{4-}$ ligands act as 8-connecting nodes. Therefore, the whole structure can thus be represented as a $(4^6)_2(4^{12}.6^{12}.8^4)$ net, as displayed in Figure 3d. The total void value of the

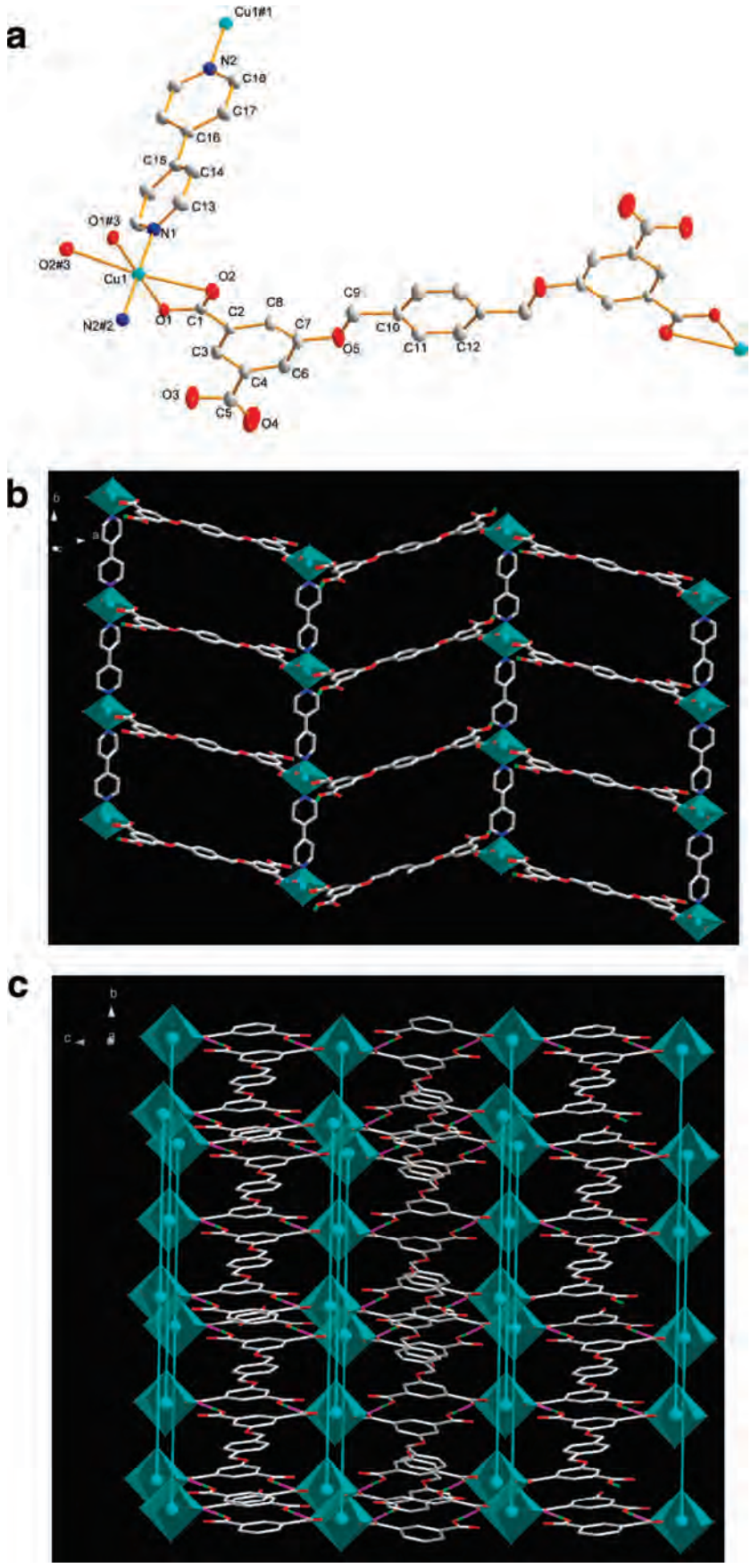

Figure 2. (a) ORTEP drawing of **3** showing 30% ellipsoid probabilities (hydrogen atoms are omitted for clarity). Symmetry codes: #1 = x, $-1 + y$, z; #2 = x; $1 + y$, z; #3 = $1 - x$, y, $0.5 - z$. (b) A 2D sheet formed in compound **3**. (Color code:white, C; red, O; blue, N; green, H; turquiose, Cu). (c) View of the 3D supramolecular network constructed from 2D sheets by hydrogen bonds in 3. Pink dotted lines represent hydrogen bonds and turquoise solid bonds represent bipy ligands (hydrogen atoms of phenyl rings are omitted for clarity; color code: white, C; red, O; green, H; turquoise, Cu).

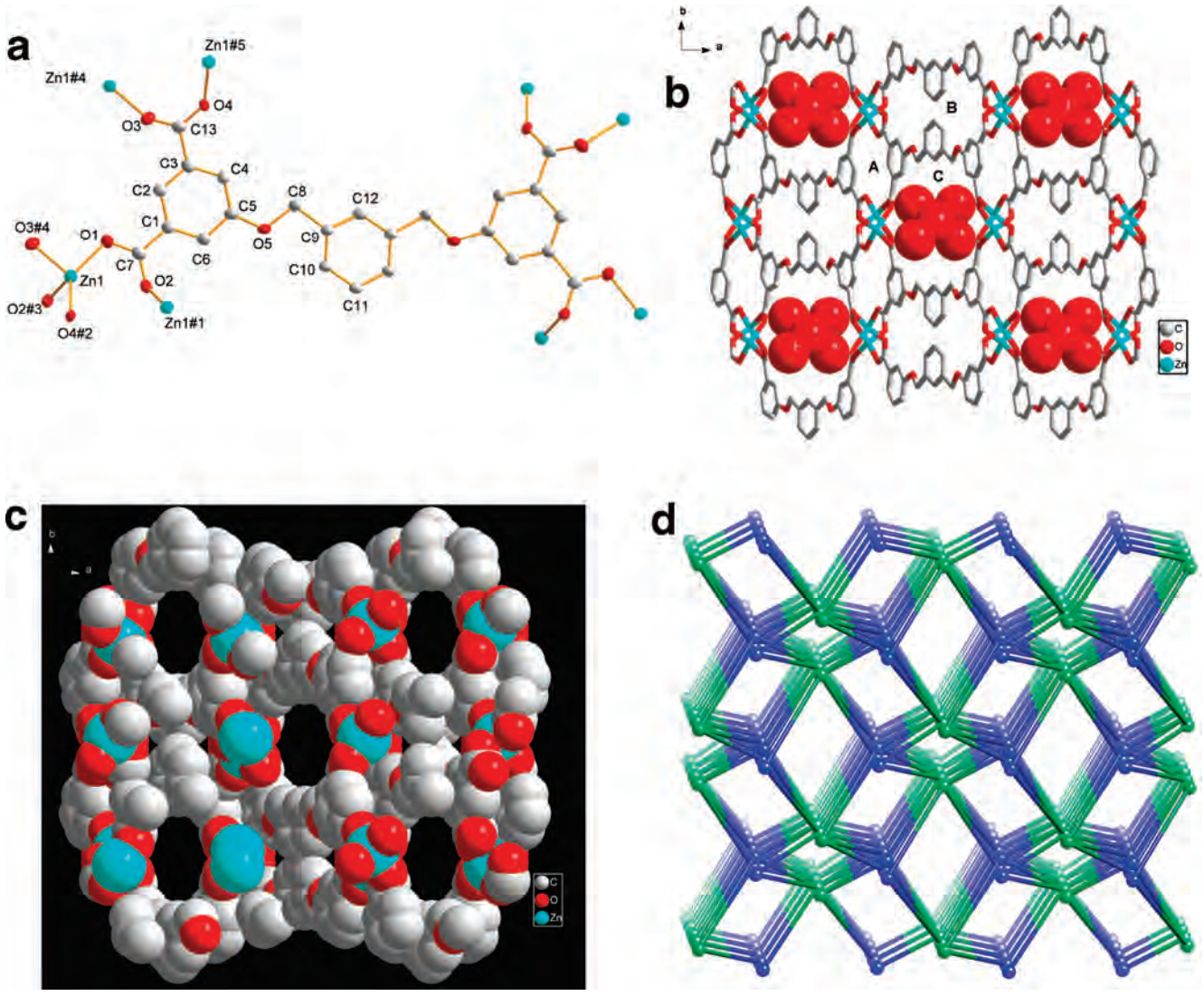

Figure 3. (a) ORTEP drawing of **4** showing 30% ellipsoid probabilities (hydrogen atoms and solvent molecules are omitted for clarity). Symmetry codes: #1 = x, $-y$, $-0.5 + z$; #2 = $0.5 - x$; $-0.5 + y$, $2.5 - z$; #3 = x, $-y$, $0.5 + z$; #4 = $0.5 - x$, $0.5 - y$, $3 - z$; #5 = $0.5 - x$, $0.5 + y$, $2.5 - z$. (b) A view of three kinds of channels of compound **4** along the c axis (hydrogen atoms are omitted for clarity). (c) Space-filling diagram showing the packing arrangement of compound **4** along the c axis (solvent molecules are omitted for clarity). (d) Schematic representation of the topology of compound **4**. Blue nodes represent Co atoms and green nodes represent $L2^{4-}$ ligands.

channels without water guests is estimated (by Platon[24]) to be 308.7 Å^3, approximately 13.4% of the total crystal volume of 2297.3(3) Å^3. All the solvent water molecules are accommodated in a disordered fashion in the channels C. To evaluate the permanent porosity of the framework of compound **4**, nitrogen sorption isotherm measurements (Supporting Information, Figure S2) were performed on a desolvated crystalline sample at 77 K. It shows a typical type-III gas sorption behavior and an N_2 uptake of approximately 20.45 cm^3 (STP)/g, with a Langmuir surface area of 9.4699 m^2/g and BET surface area of 6.7893 m^2/g.

Magnetic Properties of 1 and 2. The temperature dependence of the magnetic susceptibility of **1** in the form of $\chi_M T$ and χ_M versus T are displayed in Figure 4. At room temperature, $\chi_m T$ is equal to 6.12 cm^3·K·mol^{-1}, which is much higher than the spin-only value of 3.75 cm^3·K·mol^{-1} based on two Co(II) ions ($g = 2$ and $s = 3/2$) because of the prominent orbital contribution. Upon lowering the temperature, $\chi_m T$ continuously decreases and reaches 2.36 cm^3·K·mol^{-1} at 1.8 K. Above 120 K (Supporting Information, Figure S3), the magnetic properties of **1** obey the Curie−Weiss law and give $C = 6.50(2)$ and $\theta = -18.2(6)$

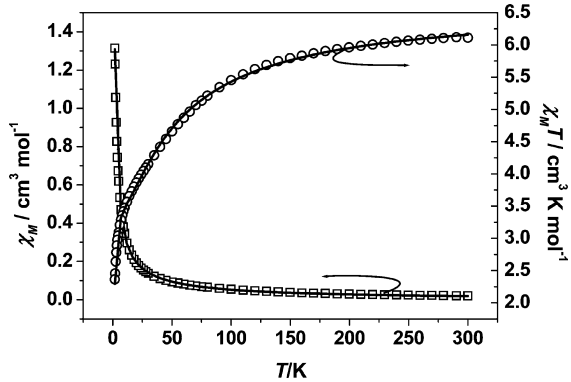

Figure 4. Temperature dependence of magnetic susceptibility in the form of $\chi_M T$ and χ_M versus T for **1**. The solid lines are the fits of the data.

(24) Spek, A. L. *J. Appl. Crystallogr.* **2003**, *36*, 7–13.

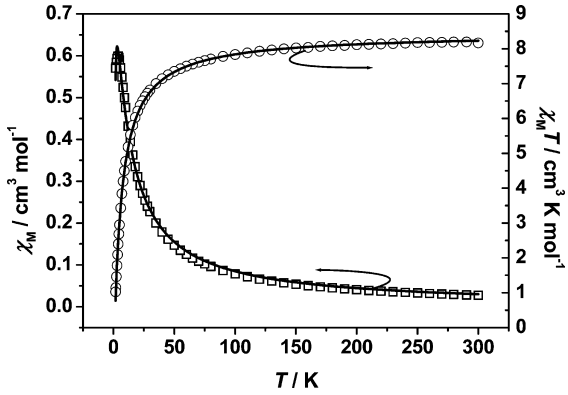

Figure 5. Temperature dependence of the magnetic susceptibility in the form of $\chi_M T$ and χ_M versus T for **2**. The solid lines are the fits of the data.

K. The obtained Weiss constant of close to −20 K for noninteracting Co^{2+} ions[25] indicates single-ion behavior of Co(II) ion above 120 K in **1**. According to the preceding structure description of **1**, no appropriate model could be used for fitting the magnetic properties of such a system. So, the treatment method reported by Rueff et al.[26] and the simple phenomenological eq 2[27] can be used here:

$$\chi_m T = A \exp^{(-E_1/kT)} + B \exp^{(-E_2/kT)} \quad (2)$$

where $A + B$ equals the Curie constant, and E_1 and E_2 represent the "activation energies" corresponding to the spin−orbit coupling and to the magnetic exchange interaction, respectively. The best fitting results give $-E_1/k = -52.4(1)$ K and $-E_2/k = -0.8(9)$ K with $C = 6.62$ cm^3 K mol^{-1}. Thus, the magnetic coupling constants between Co(II) ions are −1.78 K for **1** according to the relationship of $\chi_m T \propto \exp(+J/2kT)$.[28] This indicates that the weak antiferromagnetic exchange interaction between Co(II) ions with spin−orbital coupling of Co(II) ions dominate the magnetic properties in **1**.

The temperature dependence of the magnetic susceptibility of **2** in the form of $\chi_M T$ and χ_M versus T is displayed in Figure 5. As the temperature cools, $\chi_M T$ continuously decreases from 8.23 cm^3·K·mol^{-1} at 300 K to 1.03 cm^3·K·mol^{-1} at 1.8 K, indicating antiferromagnetic coupling between Mn ions. From the viewpoint of crystal structure, it could be presumed that the main magnetic interactions between the metal centers might happen between two carboxylate bridged Mn(II) ions, whereas the superchange interactions between Mn(II) ions through the $L1^{4-}$ ligands can be ignored because of the long length of the $L1^{4-}$ ligands. The magnetic susceptibility data were fitted assuming that the carboxylate bridges of the Mn(II) ions form an isolated spin dimer system. When the mean-field corrections zj' were taken into account, the magnetic susceptibility in the whole temperature range was fitted to eqs 3 and 4, which are deduced from the spin Hamiltonian $\hat{H} = -2J\vec{S}_1 \cdot \vec{S}_2$,

$$\chi = \frac{2Ng^2\beta^2}{kT} \times \frac{e^{2J/kT} + 5e^{6J/kT} + 14e^{12J/kT} + 30e^{20J/kT} + 55e^{30J/kT}}{1 + 3e^{2J/kT} + 5e^{6J/kT} + 7e^{12J/kT} + 9e^{20J/kT} + 11e^{30J/kT}} \quad (3)$$

$$\chi_M = \frac{\chi}{1 - (2zj'/Ng^2\beta^2)\chi} \quad (4)$$

where all symbols have their normal meanings. The best fitting gave $J = -1.94(4)$ cm^{-1} and $zj' = -0.48(1)$ cm^{-1} with a reasonable g-factor (1.96(1)), and the J value is comparable with those in carboxylate bridging Mn(II) compounds reported previously.[29] These results indicate that there exists weakly antiferromagentic interactions within the Mn_2 unit.

Luminescent Property. Luminescent compounds are currently of great interest because of their various applications in chemical sensors, photochemistry, and electroluminescent displays.[30] Previous studies have shown that coordination polymers containing zinc and cadmium ions exhibit photoluminescent properties.[31] The photoluminescent properties of free ligands and compound **4** have been investigated in the solid state at room temperature. Both ligands and compound **4** display strong violet luminescence (Figure 6, Supporting Information, Figure S4). Upon excitation at 350 nm, **4** exhibits strong fluorescent emission bands at 426 nm. The peaks of 426 nm for the compound **4** exhibit a red-shift (about 15 nm) with respect to the free H_4L2 ligand (411 nm, Figure 6). It is probably due to the decreased energy between the highest occupied molecular orbital (HOMO) and the lowest unoccupied molecular orbital (LUMO) of deprotonated $L2^{4-}$ anions by coordinating to metal centers. The high-dimensional structure of compound **4** leads to significant enhancement of fluorescence intensity compared to that of

(25) (a) Mabbs, F. E.; Machin, D. J. *Magnetism and Transition Metal Complexes*, Chapman and Hall: London, 1973. (b) Lines, M. E. *J. Chem. Phys.* **1971**, *55*, 2977–2984.

(26) (a) Rueff, J. M.; Masciocchi, N.; Rabu, P.; Sironi, A.; Skoulios, A. *Chem.—Eur. J.* **2002**, 1813–1820. (b) Rueff, J. M.; Masciocchi, N.; Rabu, P.; Sironi, A.; Skoulios, A. *Eur. J. Inorg. Chem.* **2001**, 2843–2848.

(27) Rabu, P.; Rueff, J. M.; Huang, Z. L.; Angelov, S.; Souletie, J.; Drillon, M. *Polyhedron* **2001**, *20*, 1677–1685.

(28) (a) Carlin, R. L. *Magnetochemistry*; Springer-Verlag: Berlin, Heidelberg, 1986. (b) Kahn, O. *Molecular Magnetism*; VCH: Weinheim, 1993.

(29) (a) Kim, J.; Lim, J. M.; Suh, M. C.; Yun, H. *Polyhedron* **2001**, *20*, 1947–1951. (b) Xue, D. X.; Zhang, W. X.; Chen, X. M. *J. Mol. Struct.* **2008**, *877*, 36–43. (c) Wang, M.; Ma, C. B.; Wang, H. S.; Chen, C. N.; Liu, Q. T. *J. Mol. Struct.* **2008**, *873*, 94–100. (d) Cañadillas-Delgado, L.; Fabelo, O.; Pasán, J.; Delgado, F. S.; Lloret, F.; Julve, M.; Ruiz-Pérez, C. *Inorg. Chem.* **2002**, *46*, 7458–7465. (e) Ma, C.; Chen, C.; Liu, Q.; Chen, F.; Liao, D.; Li, L.; Sun, L. *Eur. J. Inorg. Chem.* **2004**, 3316–3325. (f) Ma, C.; Wang, W.; Zhang, X.; Chen, C.; Liu, Q.; Zhu, H.; Liao, D.; Li, L. *Eur. J. Inorg. Chem.* **2004**, 3522–3532. (g) Mukherjee, P. S.; Konar, S.; Zangrando, E.; Mallah, T.; Ribas, J.; Chaudhuri, N. R. *Inorg. Chem.* **2003**, *42*, 2695–2703. (h) Fernández, G.; Corbella, M.; Mahía, J.; Maestro, M. A. *Eur. J. Inorg. Chem.* **2002**, 2502–2510. (i) Albela, B.; Corbella, M.; Ribas, J.; Castro, I.; Sletten, J.; Stoeckli-Evans, H. *Inorg. Chem.* **1998**, *37*, 788–798.

(30) (a) Wu, Q.; Esteghamatian, M.; Hu, N. X.; Popovic, Z.; Enright, G.; Tao, Y.; D'Iorio, M.; Wang, S. *Chem. Mater.* **2000**, *12*, 79–83. (b) McGarrah, J. E.; Kim, Y. J.; Hissler, M.; Eisenberg, R. *Inorg. Chem.* **2001**, *40*, 4510–4511. (c) Santis, G. D.; Fabbrizzi, L.; Licchelli, M.; Poggi, A.; Taglietti, A. *Angew. Chem., Int. Ed. Engl.* **1996**, *35*, 202–204.

(31) (a) Chen, W.; Wang, J. Y.; Chen, C.; Yue, Q.; Yuan, H. M.; Chen, J. S.; Wang, S. N. *Inorg. Chem.* **2003**, *42*, 944–946. (b) Tao, J.; Yin, X.; Wei, Z. B.; Huang, R. B.; Zheng, L. S. *Eur. J. Inorg. Chem.* **2004**, 125–133. (c) Xiong, R. G.; Zuo, J. L.; You, X. Z.; Abrahams, B. F.; Bai, Z. P.; Che, C. M.; Fun, H. K. *Chem. Commun.* **2000**, 2061–2062. (d) Zhang, J.; Xie, Y. R.; Ye, Q.; Xiong, R. G.; Xue, Z.; You, X. Z. *Eur. J. Inorg. Chem.* **2003**, 2572–2577.

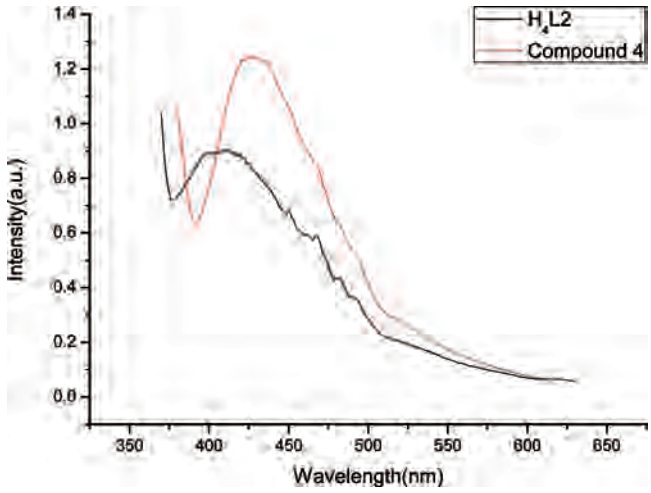

Figure 6. Solid-state photoluminescent spectra of **4** and free ligand (H_4L2) at room temperature.

the free ligand. The enhanced luminescence efficiency can be attributed to $L2^{4-}$ anions coordinated to Zn(II) ions resulting in a decrease in the nonradiative decay of intraligand excited states.[32]

Thermal Analysis and XRD Results. To characterize the compounds more fully in terms of thermal stability, their thermal behaviors were studied by TGA (Supporting Information, Figure S5). For compound **1**, a rapid weight loss is observed from 30 to 157 °C which is attributed to the loss of the coordinated water molecules, with a weight loss of 11.28% (calcd 11.04%). The TGA curve of **2** shows that **2** undergoes dehydration between 20 and 170 °C, which is again attributed to loss of the coordinated water molecules, with a weight loss of 10.71% (calcd 11.04%). The decomposition of the anhydrous residue of **1** and **2** occurs at 380 °C. In the case of **4**, a rapid weight loss is observed from 25 to 170 °C, which is attributed to the release of the lattice water with a weight loss of 4.82% (calcd 2.94%) between 20 and 170 °C. This result was unexpected, and thus we tried the measurement again upon the crystal samples, but we got the same outcome. It is thus likely that the samples adsorbed guest molecules slowly from the air at room temperature,[33] and the decomposition of the anhydrous composition occurs at 450 °C. To confirm whether the crystal structures are truly representative of the bulk materials, XRD experiments were carried out for **1**, **2**, and **4**. The XRD experimental and computer-simulated patterns of the corresponding compounds are shown in the Supporting Information, Figures S6−S8, and they show that the bulk synthesized materials and the measured single crystals are the same.

Conclusion

This contribution has described the synthesis and properties of four new compounds built from the H_4L1 and H_4L2 ligands. The results reported here will enrich the field of metal−organic frameworks based on long flexible multicarboxylate ligands. Magnetic studies reveal that both compound **1** and **2** exhibit antiferromagnetic coupling between adjacent Co(II) ions and Mn(II) ions. Compound **4** exhibits strong violet emissions and may be a good candidate for violet-light emitting materials.

Acknowledgment. This work was supported by grants from the Natural Science Foundation of China (Nos. 20571039; 20721002), National Basic Research Program of China (2007CB925103), and the Nature Science Foundation of Jiangsu province (No. BK2006124).

Supporting Information Available: Crystallographic data in CIF format, selected bond distances and angles, hydrogen bonding geometry, additional figures, TGA plots of compounds **1**, **2**, and **4**, and XRD patterns of compounds **1**, **2**, and **4**. This material is available free of charge via the Internet at http://pubs.acs.org.

IC801221R

(32) Wang, H. Y.; Gao, S.; Huo, L. H.; Ng, S. W.; Zhao, J. G. *Cryst. Growth Des.* **2008**, *8*, 665–670.

(33) Li, S. L.; Lan, Y. Q.; Ma, J. F.; Yang, J.; Wei, G. H.; Zhang, L. P.; Su, Z. M. *Cryst. Growth Des.* **2008**, *8*, 675–684.